SHOCK, Vol. 51, No. 2, pp. 235–246, 2019

OPEN

KNOCKDOWN OF TFPI-ANCHORED ENDOTHELIAL CELLS EXACERBATES LIPOPOLYSACCHARIDE-INDUCED ACUTE LUNG INJURY VIA NF-κB SIGNALING PATHWAY

Bao Q. Wang,[*§††] Meng Shi,[†§] Jian P. Zhang,[**] Xie Wu,[¶] Mei J. Chang,[*§] Zhi H. Chen,[‡] Hua H. Shen,[‡||] Yuan L. Song,[*§] Jian Zhou,[*§] and Chun X. Bai[*§||]

[*]Department of Pulmonary Medicine, Zhongshan Hospital, Fudan University, Shanghai, China; [†]Department of Cardiothoracic Surgery, Huashan Hospital, Fudan University, Shanghai, China; [‡]Department of Respiratory and Critical Care Medicine, Second Affiliated Hospital, Institute of Respiratory Diseases, Zhejiang University School of Medicine, Hangzhou, China; [§]Shanghai Respiratory Research Institution, Shanghai, China; [||]State Key Laboratory of Respiratory Disease, Guangzhou Medical University, Guangzhou, China.; [¶]Department of Nephrology, Zhongshan Hospital, Fudan University, Shanghai, China; [**]Center for Biomedical Imaging, Fudan University, Shanghai, China; and [††]Department of Pulmonary Medicine, the Central Hospital of Xuhui District, Shanghai, China

Received 9 Oct 2017; first review completed 2 Nov 2017; accepted in final form 5 Feb 2018

ABSTRACT—As activation of the coagulation system is both a consequence and contributor to acute lung injury (ALI), pulmonary coagulopathy has become a potential target for therapeutic intervention in ALI patients. We investigated the effects and possible mechanisms of endothelial cell (EC)-anchored tissue factor pathway inhibitor (TFPI) on lipopolysaccharide (LPS)-induced ALI in mice. To assess the effect of EC-anchored TFPI deletion on ALI indices, TFPI knockout (cKO) mice were generated. Mice were instilled by direct intratracheal injection LPS for the preparation of an ALI model. Evans blue dye (EBD) was injected intravenously 2 h prior to animal sacrifice (48 h post-LPS). Lungs were fixed for histopathology and the prepared tissue was homogenized or used to extract bronchoalveolar lavage fluid (BALF) or detect EBD concentration. TFPI knockdown mice with ALI were compared to wild-type (WT) mice with ALI to assess the effect of TFPI on endothelial barrier function and inflammation. TFPI deletion markedly exacerbated LPS histopathological changes in lung, and the LPS changes in protein, EBD extravasation, proinflammatory cytokines TNF-α, IL-1β, and IL-6 in BALF in lung. The number and infiltration of white blood cells (WBCs) from BALF and lung tissue of TFPI cKO mice with LPS-challenged ALI was increased compared to WT mice with LPS-challenged ALI. We also found further increased toll-like receptor 4 and nuclear factor kappa-light-chain-enhancer of activated B cells activation and additional expression of vascular cell adhesion molecule 1 and reduction of angiotensin converting enzyme 2 expression in TFPI cKO+LPS mice compared with WT+LPS mice. Endothelial-specific TFPI deficiency promoted LPS-induced pulmonary inflammation and endothelial barrier permeability possibly via toll-like receptor 4-mediated nuclear factor kappa-light-chain-enhancer of activated B cells signaling pathway activation.

KEYWORDS—Acute lung injury, coagulation endothelial cell, evans blue, tissue factor pathway inhibitor, vascular permeability

INTRODUCTION

Acute lung injury (ALI) is an important complication of many serious diseases. Inappropriate activity of leukocytes and coagulation system are key events for the development of ALI (1). Early studies have found excessive postmortem microthrombosis within damaged pulmonary microvasculature in patients with acute respiratory distress syndrome (ARDS) (2). Early after acute respiratory infection, local activation of coagulation defends against infectious agents in an attempt to trap and kill the invading microorganisms. However, coagulopathy plays an important role in the pathogenesis of lung injury and subsequent impaired pulmonary function as well (3). As activation of the coagulation system is both a consequence and contributor to ongoing lung injury, pulmonary coagulopathy has become a potential target for therapeutic intervention in ALI patients.

Tissue factor (TF), a transmembrane glycoprotein expressed on the surface of vascular smooth muscle cells, monocytes, macrophages, and endothelial cells (ECs), is believed to play a decisive role in the development of thrombotic complications (4). Activation of the extrinsic coagulation cascade through upregulation of TF-dependent procoagulant activity has been

Address reprint requests to Chun X. Bai, MD, PhD, FCCP, Department of Pulmonary Medicine, Zhongshan Hospital, Fudan University, Shanghai, China. E-mail: bai.chunxue@zs-hospital.sh.cn; Jian Zhou, PhD, Department of Pulmonary Medicine, Zhongshan Hospital, Fudan University. E-mail: zhou.jian@fudan.edu.cn; Yuan L. Song, MD, PhD, Department of Pulmonary Medicine, Zhongshan Hospital, Fudan University. E-mail: ylsong70@163.com

Funding: This work was supported by Natural Science Foundation of China (81490533, 81400018, 81570028, 81500026, 81770039), the State Key Basic Research Program (973) project (2015CB553404), the Shanghai Science and Technology Committee (15DZ1930600), the Shanghai Three-Year Plan of the Key Subjects Construction in Public Health-Infectious Diseases and Pathogenic Microorganism (15GWZK0102).

Declarations: Availability of data and material: The datasets used and/or analyzed during the current study are available from the corresponding author on reasonable request.

Authors' contributions: C.B., J.Z. and Y.S., were corresponding authors and supervised the conduction of the entire project. B.W., and M.S. were first authors and performed the research, analyzed the data, and prepared the manuscript. Z.C. and H.S. supervised coordinated the animal experiments. All authors read and approved the final manuscript.

The authors have no conflicts of interest to disclose.

DOI: 10.1097/SHK.0000000000001120

implicated in the pathogenesis of both acute and chronic lung injury and may contribute to lung inflammation (5). Tissue factor pathway inhibitor (TFPI) exerts anticoagulant activity through inhibition of the blood coagulation proteases factor TF/FVIIa/FXa complex (6). TFPI is a multidomain serine protease inhibitor consisting of three independently folded Kunitz proteinase inhibitor (KPI) domains and a highly basic C-terminal tail (7). TFPI is primarily produced by ECs, localized to an intracellular granule, and is released after cellular stimulation with thrombin. TFPI also is produced by megakaryocytes and released from activated platelets (8).

Treatment of the underlying disease and excellent supportive care using ''lung-protective'' strategies of mechanical ventilation contribute to successful clinical outcomes of ALI (9). However, specific therapies are lacking, and the cascade of events leading to ALI and ARDS, once initiated, are much less amenable to specific treatment modalities. In endotoxemic and septic animals, TF expression is increased in lung tissue. Cytokine upregulation represents the earliest response to ALI, followed by increased lung permeability, upregulation of TF, and recruitment of inflammatory cells (10). TFPI may assist in reducing mortality in animal models of severe sepsis and contribute to therapeutic effectiveness (11). Intratracheal TFPI administration improves gas exchange and prevents mortality in rats with ALI (12); however, improvement in lung function by TFPI has only been demonstrated in a relatively limited number of patients with ALI-associated sepsis and results have not been confirmed in larger, phase III clinical trials (13). Recently, our university generated mice with endothelial-specific disruption of TFPI and found that EC-specific deficiency of TFPI enhanced endothelial permeability in the lungs and facilitated metastasis in a mouse lung metastatic tumors model (14).

Pulmonary edema is a life-threatening complication characteristic of ALI and ARDS. Our data showed that TFPI is increased in bronchoalveolar lavage fluid (BALF) and decreased in lung tissue in mice with lipopolysaccharide (LPS)-induced ALI. It is possible that TFPI may contribute to the progression of ALI. Therefore, it is enormously in our interest to determine the deficiency of EC-anchored TFPI increase lung vessel permeability in ALI, considering that LPS, the toxic component of endotoxin in the outer membrane of Gram-negative bacteria, is thought to play a major role in initiating the inflammatory processes resulting in ALI/ARDS. In this report, we evaluated the effect and possible mechanisms of EC-anchored TFPI on LPS-induced ALI in mice.

MATERIALS AND METHODS

Reagents

LPS from *Pseudomonas aeruginosa* were purchased from Sigma-Aldrich (St. Louis, Mo). Rabbit anti-mouse nuclear factor kappa-light-chain-enhancer of activated B cells [NF-κB]/p65, phospho-NF-κB/p65, vascular cell adhesion molecule 1, and monoclonal antibodies were obtained from Cell Signaling Technology (Danvers, Mass). Goat anti-mouse angiotensin converting enzyme 2 (ACE2) and TFPI polyclonal antibodies were obtained from R&D Systems (Minneapolis, Minn). Mouse anti-mouse TFPI and toll-like receptor 4 (TLR4) monoclonal antibodies were obtained from Santa Cruz Biotechnology (Santa Cruz, Calif). Goat polyclonal anti-myeloperoxidase (MPO) antibodies (R&D Systems) were used for Western blotting and immunohistochemistry. The microbicinchoninic acid (BCA) protein assay reagent kit was obtained from Beyotime Biotechnology (Shanghai, China). TFPI, TNF-α, IL-1β, and IL-6 enzyme-linked immunosorbent assay (ELISA) kits were obtained from R&D Systems. TF ELISA kits were obtained from the Abcam Company (Cambridge, UK).

Mouse experimental protocol and tissue collection

Mice (8-week-old mice) were housed in cages with access to food and water in a temperature-controlled room with a 12 h dark/light cycle (six mice per cage). Regular rodent chow and tap water were available *ad libitum*. The Institutional Animal Care and Use Committee of Fudan University, People's Republic of China, approved all experiments and animal care procedures. Wild-type (WT) mice were purchased from SLAC Laboratory Animal Center in Shanghai. The generation of homozygous TFPI floxed mice ($TFPI^{flox/flox}$/Tek) has been previously described (14). These mice were maintained on a C57BL/6 background. Eight-week-old $TFPI^{flox/flox}$/Tek mice, sex- and-age matched WT C57BL/6 mice, and $TFPI^{flox/flox}$ littermates were used in this study. Mice were anesthetized with intraperitoneal injections of sodium pentobarbital and instilled by direct intratracheal injection of 2.5 μL/g of 2 mg/mL LPS or 2.5 μL/g of phosphate buffer saline (PBS) (control) for selected experiments. After 48 h, mice were anesthetized for plasma, BALF, or lung histological analysis. A transcardial puncture was performed. Six hundred fifty microliters of whole blood was taken from the left ventricle in a 1-mL syringe. Blood was collected into 3.2% citrate (9:1 ratio) and centrifuged within 2 h. BALF was obtained by instilling 500 μL pre-cooling PBS and gently aspirating three times from the left lung by cannulating the exposed trachea with a 22G-feeding needle tied with surgical thread. BALF fluid was assessed for cell counts, protein content, and Evans blue dye (EBD) and cytokine levels. Lung tissue was flash frozen in liquid nitrogen and stored at −80°C.

Blood collection and sample preparation

Platelet-poor plasma (PPP) was prepared by two sequential centrifugations to remove residual platelets. Citrated blood was first centrifuged 6,000 *g* for 5 min at 4°C; supernatant was then centrifuged at 10,000 *g* for 5 min at 4°C to prepare PPP in less than 2 h, which was aliquoted and stored at −80°C until used (15).

Coagulation assays

Arterial blood samples were collected in tubes containing one-tenth the volume of 3.2% sodium citrate to measure activated partial thromboplastin time (APTT), prothrombin time (PT), and thrombin time (TT). APTT, PT, and TT were measured with the appropriate reagents (Siemens Healthcare Diagnostics Products, Marburg, Germany) using a semiautomated coagulation analyzer (Stago Diagnostica, Asnieres, France). APTT was measured by incubating 100 μL of PPP with 100 μL of APTT reagent for 180 s; coagulation was triggered by adding 100 μL of 25 mM $CaCl_2$ at 37°C. PT was measured by incubating 100 μL of plasma for 60 s at 37°C, followed by the addition of 200 μL of pre-warmed thromborels. TT was measured by incubating 100 μL of plasma and 200 μL of TT reagent buffer for 1 min at 37°C. Data points represent the mean of duplicate measurements.

Lung wet-to-dry weight ratio

Lung wet/dry weight ratios were used to determine the extent of pulmonary edema caused by LPS and TFPI deletion. Cardiac lobe and diaphragmatic lobe of the right lung were removed and placed on a piece of preweighed aluminum foil. The lung was weighed and placed in a 65°C oven for 5 days. The dry weights were monitored until two successive weights were similar. The lung was weighed again and the ratio was calculated ([lung before drying]/[lung after drying]).

Inflammatory cell counts in BALF

BAL was centrifuged at 400 *g* for 10 min at 4°C and the cell-free supernatant was collected and frozen at −80°C for cytokine assay. Total BAL protein was measured in the cell-free supernatant according to the manufacturer's protocol. After supernatants were removed, cell pellets were re-suspended in 100 μL PBS after treatment with red blood cell lysis buffer. Total cell counts were performed in cell suspensions with an animal hemacytometer. Ten microliters of remaining cell suspensions were used to prepare cytosmears by dripping the solution onto glass slides. Smears were air-dried overnight prior to staining with Wright's stain to observe nucleated cells.

Morphological evaluation of lung sections

For morphological evaluation, lungs were removed and fixed in 10% buffered formalin, embedded in paraffin wax, and sectioned at 4 μm. Sections were stained with hematoxylin and eosin (H&E). Severity of lung injury was

semiquantitatively assessed as described previously with slight modifications (16). All histologic examination was carried out in a double-blind manner under 100× magnification. Five images of each tissue sample were captured at 100× power. Pathological features were determined as follows: (i) focal alveolar membrane thickening; (ii) capillary congestion; (iii) intra-alveolar hemorrhage; (iv) interstitial; and (v) intra-alveolar neutrophil infiltration. Each feature was scored from 0 to 3 based on its absence (0) or presence to a mild (1), moderate (2), or severe (3) degree, and a cumulative total histology score (THS) was determined. The scores for each parameter were averaged across the five images and averages were obtained as the mean THS for the sample.

Radiological analysis

In the past decade, micro-computed tomography (CT) has become a powerful technique in laboratory investigation as technical advances in computer speed and memory have enabled micro-CT systems to generate high-spatial-resolution images of small specimens (17). To evaluate LPS responses to ALI, micro-CT images were obtained of the entire thorax using a Siemens Inveon micro-CT scanner (Siemens, Germany) after 48 h of LPS administration. The mice were anesthetized and placed on a plate in the supine position. CT images were collected on a volumetric CT scanner at 70 kVp and 500 μA. Images were acquired at 1,300 ms per frame and 360 views, and were reconstructed using the Feldkamp Algorithm. The reconstructed image was 2,048 × 2,048 pixels and effective pixel size was 39.99 μm. The final reconstructed data were converted to the Digital Imaging and Communications in Medicine format (Lucion; MeviSYS, Seoul, Korea).

ELISA for mouse TFPI and inflammatory cytokine analysis

Mouse Quantikine ELISA kits were from R&D Systems, and were used to analyze TNF-α, IL-1β, and IL-6 in BAL fluid supernatants according to the manufacturer's instructions. The protein levels in plasma, BALF, and lung tissue were assessed using DuoSet ELISA Development kits for mouse TFPI (R&D Systems) according to the manufacturer's instructions. Cytokine and TFPI content in plasma and BALF were determined by multiplying cytokine and TFPI concentration (pg/mL). TFPI and TF content in total protein of lung tissue were determined by TFPI and TF concentration. The soluble TF in BALF was measured using a mouse TF ELISA performed according to the manufacturer's instructions.

EBD leakage

Quantifying the amount of albumin conjugated to EBD fluxing across organ-specific vascular barriers is a popular technique to assess endothelial monolayer integrity in murine models of human disease. Forty-eight hours after LPS intratracheal instillation, groups were injected via the tail vein with 2% solution of Evans blue in normal saline (20 mg/kg); 2 h after injection, BALF was performed and the left lung lobe was removed and immersed in formamide solution at 65°C. After 72 h of incubation, formamide, including extracted EBD, was collected, and the lung in formamide solution was placed on a piece of preweighed aluminum foil in a 65°C oven for 5 days. The lung was weighed again and the dry lung weight was calculated. The absorbance at 630 nm was measured with BAL fluid supernatants and formamide samples using a spectrophotometer. A standard curve was prepared in the same solution (linear in the range 0.1–500 μg/mL), and the corresponding values were read by inverse prediction of the regression equation describing the standard curve. The EB concentration read in μg/mL was converted to μg/g dry weight of the removed left lung (18).

Histology, immunohistochemistry, and immunofluorescence

Histological and immunohistochemical procedures were performed as previously described. Immunohistochemistry, paraffin sections were de-waxed, hydrated through a descending ethanol series, washed in 0.05 M Tris-HCl buffer, pH 7.6, and placed in boiling citrate buffer (pH 5.8,) for 10 min and allowed to cool at room temperature for 20 min. They were rinsed 3× in PBS (pH 7.8) for 4 min each. Slides were placed in 50 mL of 0.5% trypsin solution, incubated in a water bath at 37°C for 15 min, and rinsed 2× Tris HCl (pH 7.8) for 4 min each. After rinsing, slides were washed 2× in PBS (pH 7.6) for 4 min each, then blocked in 10% lamb serum for 30 min at room temperature, followed by incubation with primary antibody overnight at 4°C. After washing 3× with PBS for 15 min, secondary antibodies were applied for 20 min at 3°C. In brief, lungs were embedded in paraffin and 4 μm serial sections (300 μm apart) were obtained. Immunohistochemical detection was performed by incubating sections with corresponding primary and secondary antibodies. For immunofluorescence staining, lung tissues were treated with 1% Triton, blocked in 5% bovine serum albumin, and then exposed to anti-TFPI mouse at a 1:100 dilution in antibody diluent overnight at 4°C. Slides were incubated with Alexa-Fluor488-coupled goat anti-mouse secondary antibodies at 1:300 dilution for 1 h before nuclear counterstaining with 2-(4-Amidinophenyl)-6-indolecarbamidine dihydrochloride and mounting.

Extraction of proteins and Western blot analysis

Protein extracts were prepared from lung tissues. Lungs from each of group were dissected out and immediately flash frozen in liquid nitrogen. Frozen tissue was ground into a fine powder and homogenized in 10 volumes of protein extraction buffer. The tissue homogenate was centrifuged at 14,000 *g* for 5 min at 4°C. The supernatant was then collected and protein concentration was determined. Samples containing equal protein amounts (20 μg) were electrophoresed on 10% or 12% Sodium dodecyl sulfate polyacrylamide gel electrophoresis for detection of MPO, NF-κB, vascular cell adhesion molecule 1 (VCAM-1), ACE2, TLR4, and TFPI, and transferred to polyvinylidene difluoride membranes for Western blot analysis. The relative protein expressions levels were normalized to those of actin. The membranes were blocked in 5% nonfat dry milk in 0.1% Tween 20 in Tris-buffered saline and were incubated overnight with primary antibody incubation. The blots were then incubated with anti-goat, anti-rabbit, or anti-mouse IgG horseradish peroxidase-conjugated antibodies (Beyotime Biotechnology) at a 1:2,000 dilution at room temperature for 1 h. Peroxidase activity was revealed with the Amersham ECL plus Western blot detection reagents (Beyotime Biotechnology). Data are representative of three independent experiments. Densitometric analysis of the bands was carried out using Image J software (National Institutes of Health, Bethesda, Md).

Statistical analysis

Data are expressed as mean ± standard deviation of six independent experiments if normally distributed and as median (interquartile range) when non-normally distributed. Differences between groups were compared using unpaired student's *t*-tests. For multiple-group comparisons, a one-way ANOVA, followed by the *post-hoc* Tukey test was used; $P < 0.05$ was considered statistically significant. Statistical analyses were performed using GraphPad Prism6 (Prism, Version 6, La Jolla, Calif).

RESULTS

Generation and evaluation of TFPI cKO mice

We generated an endothelial-specific disruption of TFPI mouse line (*Tek-Cre;LoxP-TFPI* mice) through the crossbreeding of *B6.Cg-Tg (Tek-cre)* mice with *B6.Cg-Tg (LoxP-TFPI)* mice (Fig. 1A). Mice were indistinguishable from their littermates. To determine genotyping of the offspring, genomic DNA isolated from the murine tail of weanling animals was subjected to PCR (Fig. 1B). To evaluate the efficiency of the TFPI knockout, Western blot and ELISA were used to analyze lung TFPI protein expression. Western blot revealed that TFPI protein was 28% of that of WT mice ($P = 0.0029$; Fig. 1C); ELISA showed that TFPI concentration was 13.9% of that of WT mice ($P < 0.0001$; Fig. 1D-a). The TFPI concentration of $TFPI^{fl/fl}$/Tek mice in BALF was 29% of that of WT mice ($P < 0.0001$; Fig. 1D-b). We measured TFPI concentration in plasma using ELISA and found that plasma TFPI concentrations in TFPI cKO mice were 91.8% lower than in WT mice ($P < 0.0001$; Fig. 1D-c). Immunofluorescence showed that TFPI protein was absent in lung sections of TFPI cKO mice but present in WT mice (Fig. 1E).

Coagulative function and TFPI concentration in TFPI cKO mice with ALI

The coagulation variables TT, APTT, and PT were measured in plasma in three different strains of mice using semiautomated coagulation analyzer (Stago Company, France). The results showed that PT, TT, and APTT were not significantly difference ($P > 0.05$) across experimental groups (Fig. 2A).

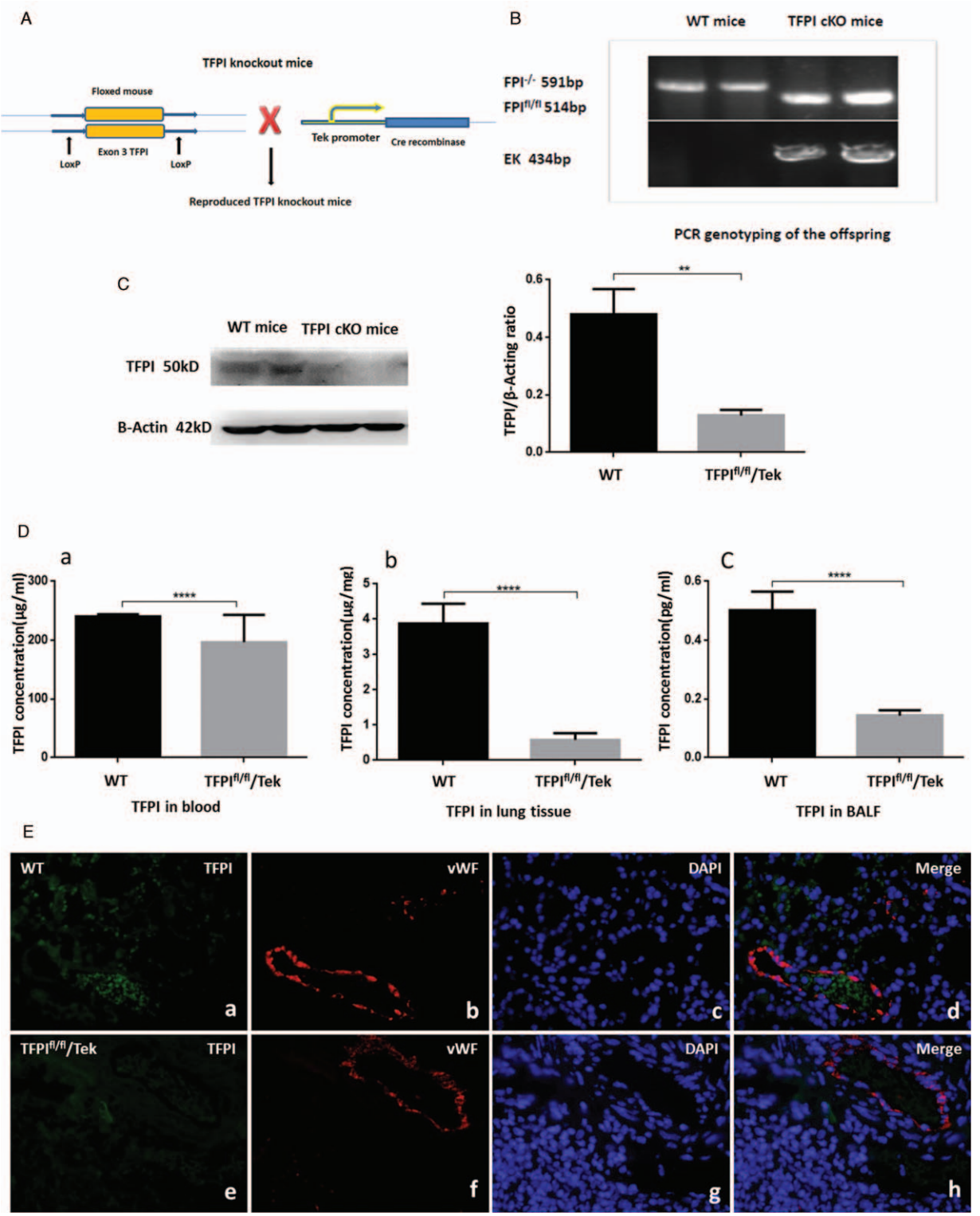

Fig. 1. **Generation of TFPI$^{fl/fl}$/Tek mice.** (A) Schematic representation of endothelial deletion of the *TFPI*; X represents breeding. (B) Recombination of the *TFPI^{loxP}* allele and Tek was examined in the tail of TFPI$^{fl/fl}$/Tek mice and WT mice, as determined by PCR and agarose gel electrophoresis; (C) Expression of TFPI in lung tissue was determined by Western blot; expression of TFPI was determined by densitometry; (D) TFPI expression was examined by ELISA in the blood, BALF, and lungs of the TFPI$^{fl/fl}$/Tek mice and WT mice; (a) TFPI concentration (pg/mL) in blood; (b) TFPI concentration (pg/mg) in lung tissue; (c) TFPI concentration (pg/mL) in BALF; (E) Immunofluorescence stainings of lung tissue TFPI from WT (a-d) and TFPI cKO mice (e-h) are shown at 400× magnification; (a, e) TFPI staining; (b,f) vWF fluorescence; (c, g) DAPI staining; (d, h) merged images. The data are presented as mean ± SD, Statistically significant differences are denoted by asterisks: $^{*}P < 0.05$, $^{**}P < 0.01$, $^{***}P < 0.001$, $^{****}P < 0.0001$. BALF indicates bronchoalveolar lavage fluid; DAPI, 2-(4-Amidinophenyl)-6-indolecarbamidine dihydrochloride; ELISA, enzyme-linked immunosorbent assay; PCR, polymerase chain reaction; TFPI, tissue factor pathway inhibitor; WT, wild-type.

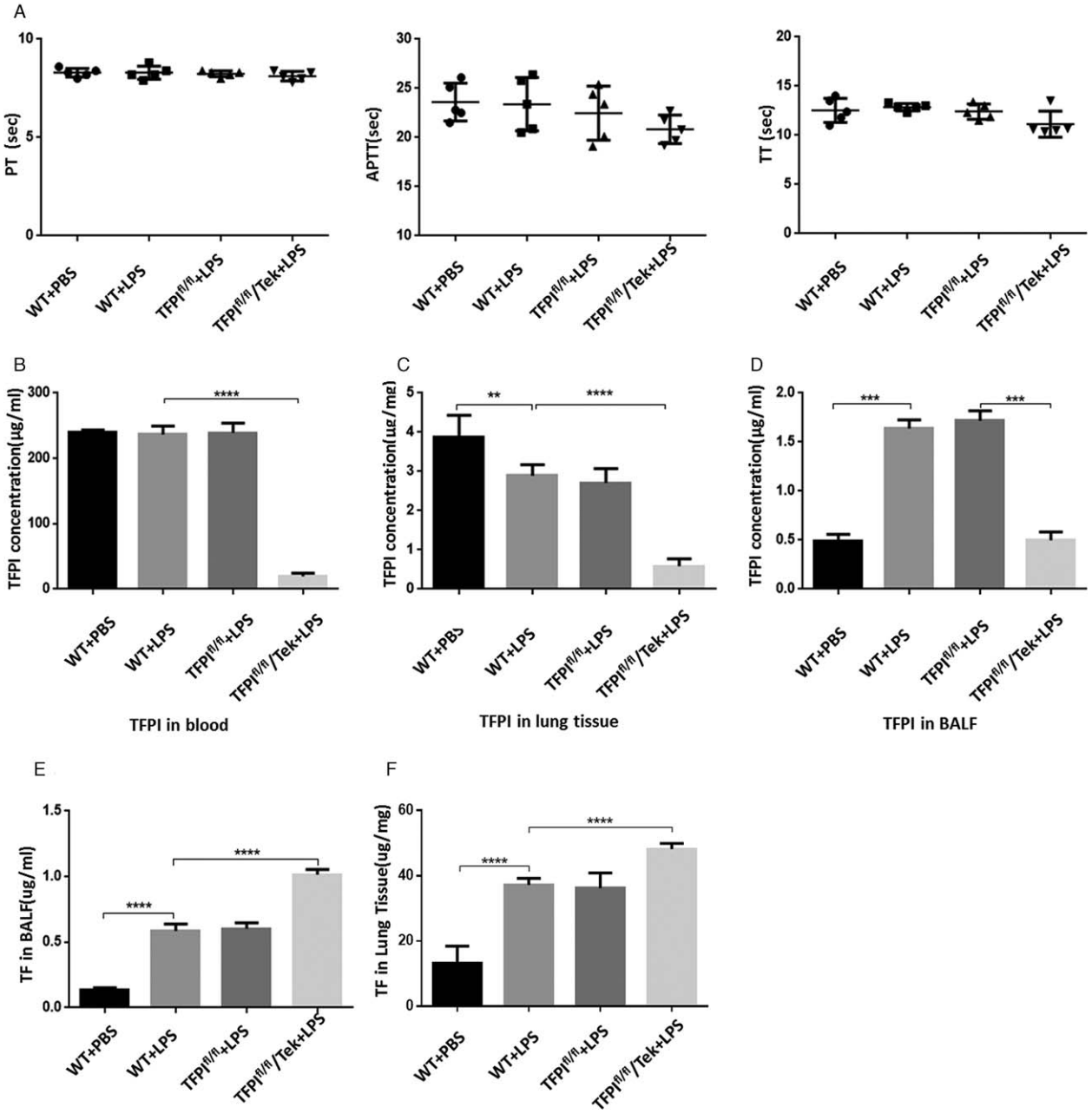

FIG. 2. **Coagulative function and TFPI concentration in TFPI cKO mice with ALI.** WT mice, $TFPI^{fl/fl}$ mice, and $TFPI^{fl/fl}$/Tek mice were sacrificed 48 h after LPS injection via endotracheal instillation. Data were obtained within 2 h after collecting blood, BALF, and lungs from mice and are presented as mean ± SD (n = six per group); compared to control: $^{*}P < 0.05$; $^{**}P < 0.01$; $^{***}P < 0.001$; $^{****}P < 0.0001$. (A) APTT: activated partial thromboplastin time; PT: prothrombin time; plasma coagulation time TT: thrombin time; (B) TFPI concentration (pg/mL) in blood using ELISA; (C) TFPI concentration (pg/mg) in lung tissue using ELISA; (D) TFPI concentration (pg/mL) in BALF using ELISA; (E) TF concentration (μg/mg) in lung tissue applying a kinetic ELISA; (F) TF concentration (μg/mL) in BALF applying a kinetic ELISA. ALI indicates acute lung injury; BALF, bronchoalveolar lavage fluid; ELISA, enzyme-linked immunosorbent assay; TF, tissue factor; TFPI, tissue factor pathway inhibitor; WT, wild-type.

Coagulation function parameters were also not significantly different in LPS-treatment mice. TFPI concentrations were measured using ELISA in the BALF, plasma, and lung homogenates of six mice of each experimental groups in order to determine if variation of TFPI expression was associated with LPS-induced lung injury. Forty-eight hours after ALI, concentrations of TFPI in BALF increased in both TFPI cKO mice (502 ± 63pg/mL) and WT mice (1,638 ± 89 pg/mL) compared to sham-treated mice (TFPI cKO mice: 143 ± 7 pg/mL in; WT mice: 501 ± 26 pg/mL) ($P < 0.05$; Fig. 2D). Concentrations of TFPI in lung tissue decreased in both TFPI cKO mice (584 ± 188 pg/mg) and WT mice (2,890 ± 280 pg/mg) compared with sham- treated mice (WT mice: 3,872 ± 566 pg/mg) ($P < 0.05$; Fig. 2C). TFPI protein levels in BALF were significantly increased after LPS infusion due to the high levels of protein in BALF. However, TFPI plasma concentrations in WT and $TFPI^{fl/fl}$ mice after ALI were not significantly higher than sham-treated WT mice (Fig. 2B). To define the expression of

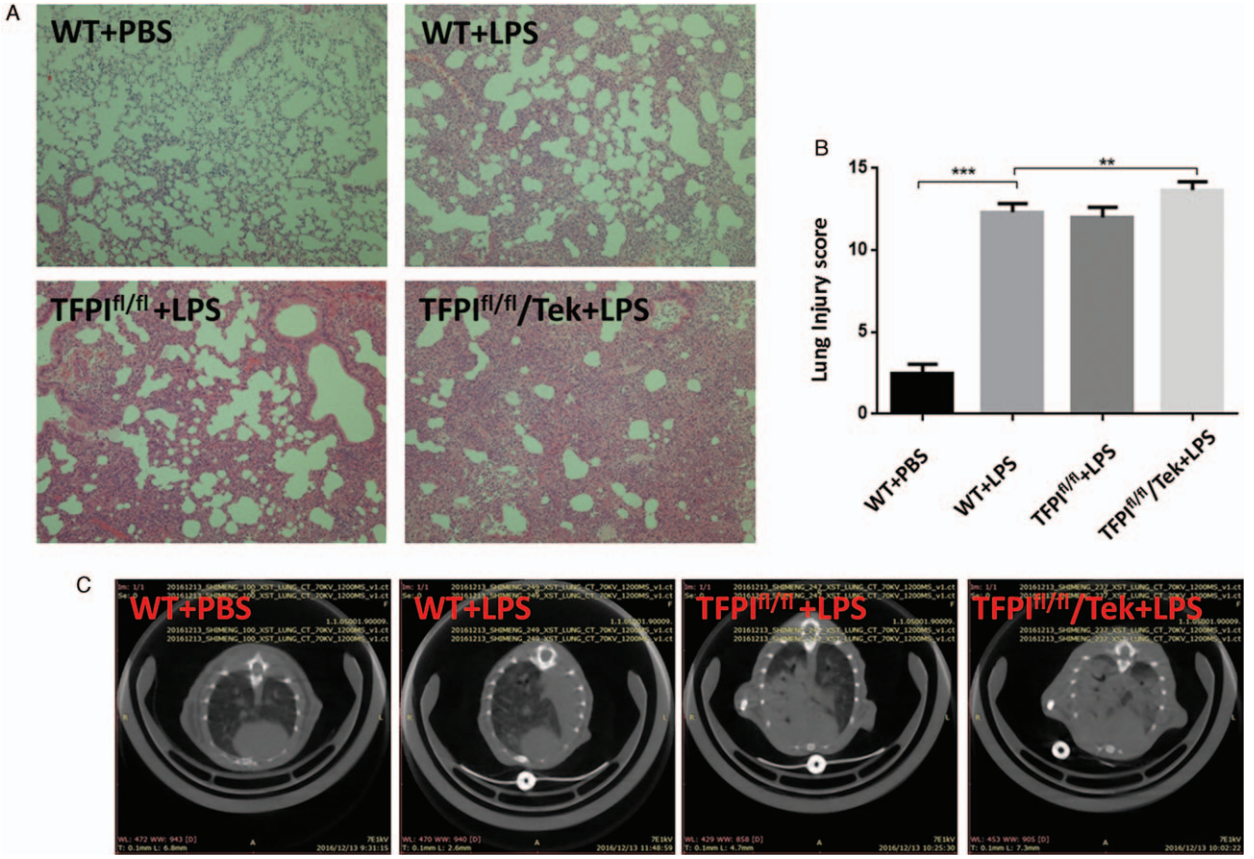

FIG. 3. **Endothelial TFPI deletion exacerbated lung pathological changes in LPS-induced ALI mice.** WT mice were intratracheally instilled with PBS control and LPS. TFPI$^{fl/fl}$ and TFPI$^{fl/fl}$/Tek mice were intra-tracheally instilled with LPS; (A) Representative 4–5um-thick section (H&E stained) of one of six mice per treatment group is shown at 100× magnification. (B) Mean semiquantitative distribution of THS of lung injury in mice (n = 6 mice per group); error bars represent SD; statistically significant differences are denoted by asterisks: $^{*}P < 0.05$; $^{**}P < 0.01$; $^{***}P < 0.001$; $^{****}P < 0.0001$; (C) Microcomputed tomography images of transverse sections showing lung injury severity in each treatment group. ALI indicates acute lung injury; BALF, bronchoalveolar lavage fluid; LPS, lipopolysaccharide; PBS, phosphate buffer saline; TFPI, tissue factor pathway inhibitor; WT, wild-type.

TF in LPS-induced ALI and TFPI cKO mice, TF concentrations were measured in lung homogenates and BALF by applying a kinetic ELISA (Fig. 2, E and F).

Endothelial TFPI deletion exacerbated lung pathological changes in LPS-induced ALI mice

We determined the effects of TFPI deletion on lung pathological changes in LPS challenged mice. Lung histology showed that LPS produced remarkable lung inflammatory responses, including significant interstitial infiltration of inflammatory cells, intra-alveolar hemorrhage, capillary congestion, and thickening of alveolar walls. Severity of lung injury was semiquantitatively assessed using THS (Fig. 3B). The pathological changes in the lungs were significantly aggravated in the knockout of endothelial TFPI mice ($P < 0.01$; Fig. 3, A and B). LPS administration induced significant inflammatory responses in the lungs of WT and TFPI$^{fl/fl}$ mice compared to WT control mice ($P < 0.001$; Fig. 3A). Micro-CT revealed bilateral patchy infiltrates in LPS-induced WT mice (Fig. 3C), in contrast with the normal radiological aspect of the lungs in the control group. Infiltrates and injury were more prominent in the lungs of the TFPI$^{fl/fl}$/Tek mice.

Endothelial TFPI deletion increased vascular permeability in ALI

Lung endothelial barrier dysfunction is characterized by increased permeation of fluid and macromolecules into the interstitium and alveolar space in ALI. An increase in wet-to-dry ratio is an indication of fluid accumulation in the lungs (Fig. 4A). The wet-to-dry ratio was 4.4 ± 0.04 in control WT animals and 4.7 ± 0.1 in WT+LPS mice. LPS consistently induced a significant increase in the total protein concentration in BALF (Fig. 4). Total protein (mg/mL) in BALF was 5.8 ± 1.3 in control WT mice and increased to 15.6 ± 2.7 after LPS-induced ALI across 48 h. LPS injection caused infiltration of Evans Blue-stained albumin from the vessel into lung tissue, further substantiating the effect of LPS on EC barrier dysfunction (Fig. 4, C and D). Total EB dye in BALF and in the control lungs was 3.89 ± 0.7 (μg/mL) and 1.70 ± 0.9 (μg/g), respectively, and the relative amounts increased to 16.2 ± 0.8 (μg/mL) and 4.07 ± 0.65 (μg/g) in WT+LPS mice, respectively.

Lung injury was analyzed in both WT and TFPI cKO mice challenged with LPS. Following PBS treatment, lung injury and vascular permeability were not different between in WT and TFPI cKO mice (data not shown). Following LPS treatment, the lung wet-to-dry ratio and BALF protein levels were higher in

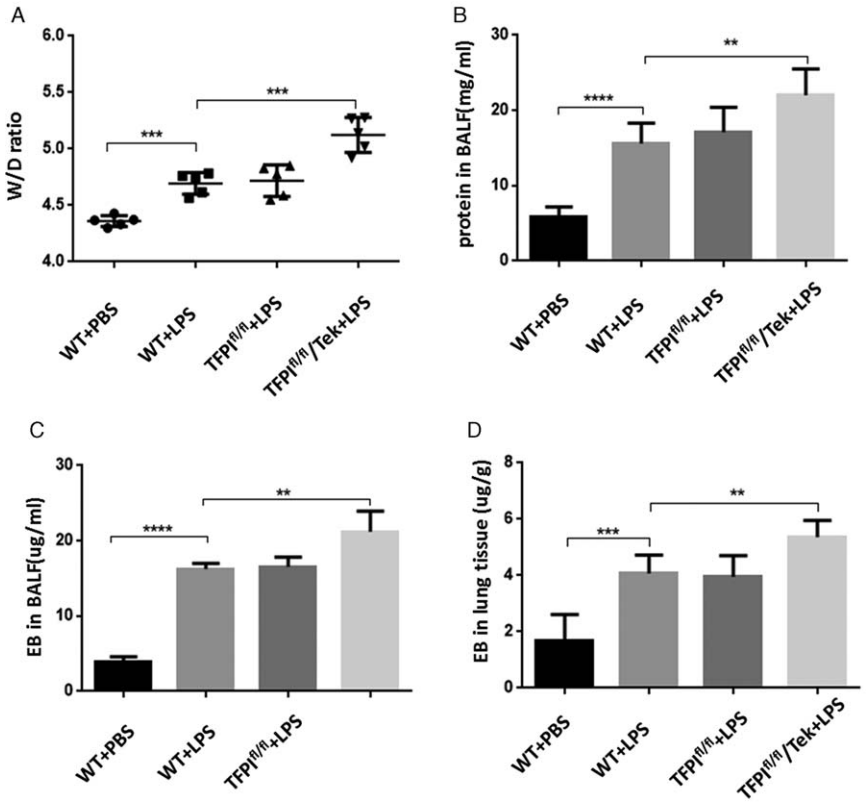

FIG. 4. **Endothelial *TFPI* deletion increased vascular permeability in ALI.** (A) Wet-to-dry lung weight ratio (W/D) was calculated after LPS induction, and left lung tissues were separated and placed on tinfoil to measure their wet weight. The tissues were then placed in a 65°C thermotank for 5 days to obtain dry weight. Compared to the WT+PBS group, the W/D value increased significantly in each LPS-induced lung injury group, respectively; (B) BALF was collected after treatment and centrifuged. Protein content was estimated in the clear supernatant using a bicinchoninic acid (BCA) protein assay kit. Endothelial *TFPI* deletion increased total protein accumulation in the BALF of mice with LPS-induced lung injury; (C, D) Mice were injected with an Evans blue solution via tail vein 2 h before termination. Evans blue was measured in BALF (C) and whole left lung formamide liquid (D) in WT, $TFPI^{fl/fl}$, and $TFPI^{fl/fl}$/Tek mice. EB values were increased in each LPS-induced lung injury group compared with the WT control group. These indicators were exacerbated in the TFPI cKO mice in the ALI group; data are presented as mean ± SD; statistically significant differences are denoted by asterisks: $^{*}P < 0.05$; $^{**}P < 0.01$; $^{***}P < 0.001$; $^{****}P < 0.0001$. ALI indicates acute lung injury; BALF, bronchoalveolar lavage fluid; LPS, lipopolysaccharide; PBS, phosphate buffer saline; TF, tissue factor; TFPI, tissue factor pathway inhibitor; WT, wild-type.

TFPI cKO mice than in WT mice (Fig. 4, A and B). Consistent with this finding, total EBD in BALF and the lungs were also higher, especially in the TFPI cKO mice (Fig. 4, C and D).

Inflammatory cell accumulation and lung inflammatory response were enhanced in TFPI cKO mice after ALI

Assessment of total WBC count in BALF using Giemsa staining (100×) showed that the number of cells in air spaces increased dramatically in response to LPS stimulation (Fig. 5, A and B). The inflammatory effects of TFPI cKO were evaluated by measuring cells in BALF of ALI mice. A nearly eight-fold increase in BALF cellular counts in ALI mice compared with control mice was found; the total number of BALF cells increased significantly by 50% in the TFPI cKO+LPS group compared with the WT+LPS group.

The severity of lung injury and inflammation were monitored by measuring MPO activity in lung tissue. LPS significantly increased MPO activity in tissue homogenates. An increased concentration of MPO in lung tissue is suggestive of neutrophil activation by Western blot (Fig. 5, C and D). MPO was evaluated using immunohistocytochemical criteria (Fig. 5E). Pulmonary myeloperoxidase expression was extremely low in PBS-exposed mice; however, LPS-exposed mice had dramatic increases in lung myeloperoxidase compared to PBS-infused mice. MPO levels were also increased in LPS-treated TFPI cKO mice.

We measured TNF-α (Fig. 5F), IL-1β (Fig. 5G), and IL-6 (Fig. 5H) using ELISA to study the inflammatory response in lung tissues. IL-1β, IL-6, and TNF-α levels in BALF were significantly higher in the LPS group than in the PBS group. Comparison of cytokine concentrations in BALF between LPS-treated WT mice and LPS-treated TFPI cKO mice revealed significantly elevated levels of TNF-α ($P < 0.05$), IL-1β ($P = 0.01$), and IL-6 ($P = 0.014$) in LPS-treated TFPI cKO mice. The increased levels of TNF-α, IL-1β, and IL-6 caused by LPS administration were further promoted by endothelial-anchored TFPI knockdown.

Endothelial-specific disruption of TFPI destroyed endothelial gaps by activating TLR4-mediated NF-κB activity after ALI

To explore the mechanisms associated with the deterioration of ALI in TFPI cKO mice, we evaluated two important targets in ECs and the ACE2, VCAM-1, and TLR4-mediated NF-κB

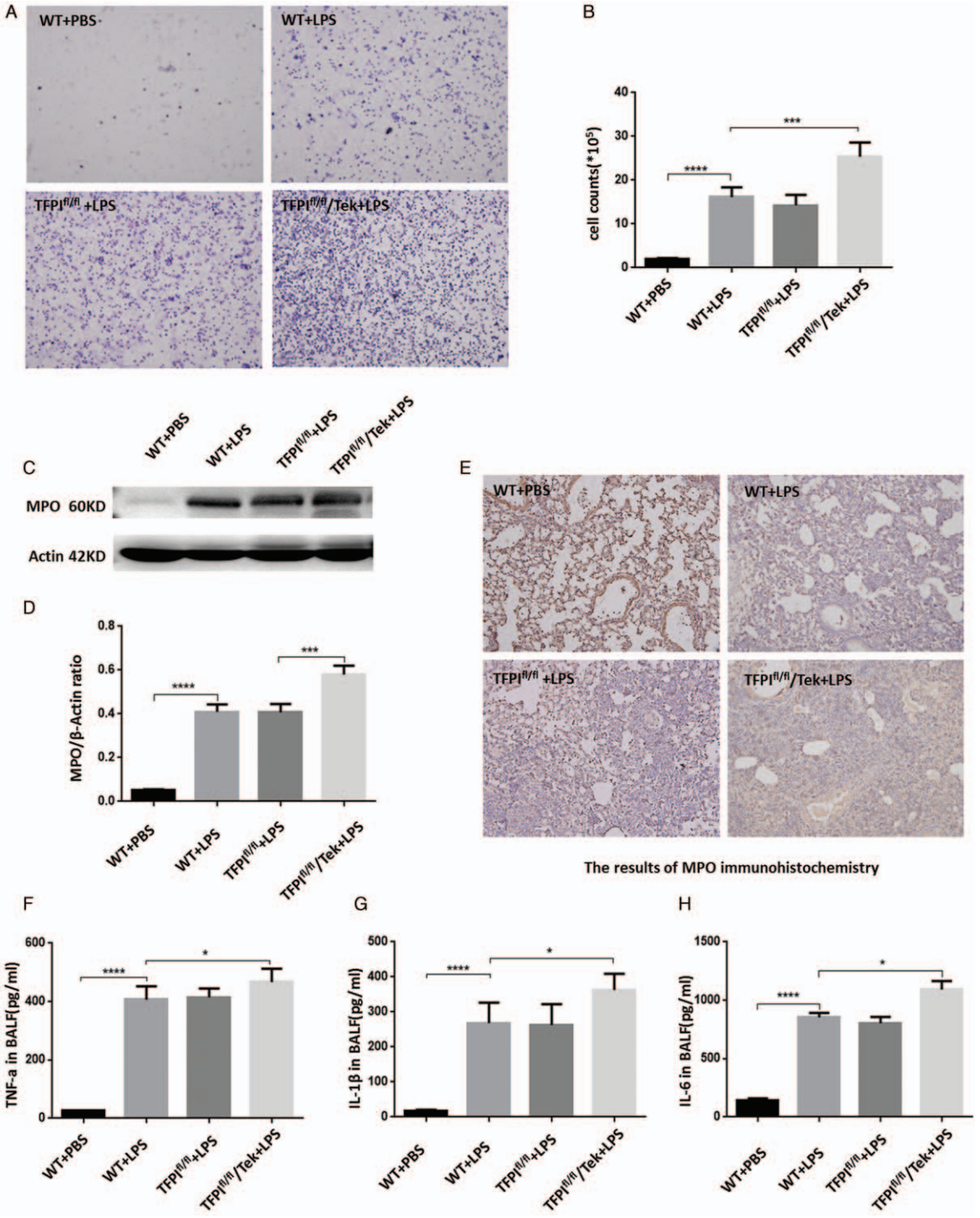

FIG. 5. **Accumulation of inflammatory cells and lung inflammatory response were enhanced in *TFPI* cKO mice after ALI.** To confirm that the inflammatory response was aggravated in TFPI cKO mice compared with WT mice, we measured cell number and cytokines in the BALF and MPO activity in lung tissue. (A) Representative images of May-Grünwald-Giemsa stained cells from BALF of differentially treated mice (100× magnification); (B) Total BALF cellular counts in BALF; (C, D) MPO activity in lung homogenates by Western blot; (E) Representative images of immunohistochemical staining for MPO in different treatment groups; (F) BALF TNF-α; (G) BALF IL-1β (H)BALF IL-6; data are presented as mean ± SD; statistically significant differences are denoted by asterisks: $^{*}P < 0.05$; $^{**}P < 0.01$; $^{***}P < 0.001$; $^{****}P < 0.0001$. ALI indicates acute lung injury; BALF, bronchoalveolar lavage fluid; LPS, lipopolysaccharide; PBS, phosphate buffer saline; TF, tissue factor; TFPI, tissue factor pathway inhibitor; WT, wild-type.

signaling pathways, which play key roles in LPS-induced lung injury. Recently, it has been shown that ACE2 treatment has therapeutic effects on ALI-induced increases in lung vessel permeability through different mechanisms (19). ACE2 protein expression was downregulated in WT mice after ALI. The TFPI cKO ALI model suggests that ALI induced by LPS resulted in more severe injury and decreased ACE2 expression (Fig. 6, B and C) and immunehistochemical staining (Fig. 6A). VCAM-1

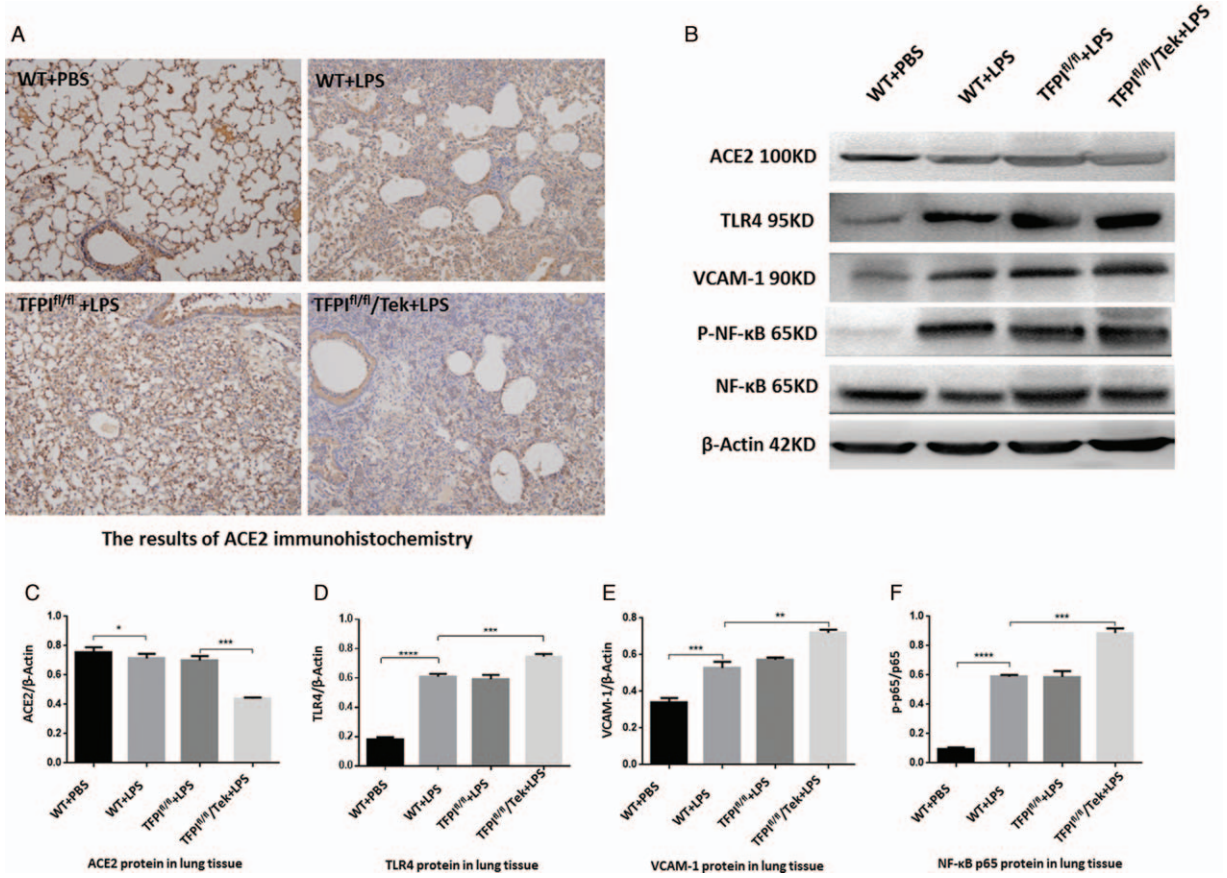

FIG. 6. **Endothelial-specific disruption of TFPI destroyed endothelial gap by activation of NF-κB activity after ALI ACE2 plays a critical role in LPS-induced ALI.** (A) Downregulated ACE2 expression in the lungs of the LPS group. Immunohistochemical staining showed decreased ACE2 expression; (B) ACE2, TLR4, VCAM-1, NF-κB, and p-NF-κB protein expression in lung tissue samples was evaluated by Western blot. Membrane probing with actin was used as a normalization control; (C) Expression of ACE2 in lung tissue homogenates prepared from control and LPS-treated mice were analyzed by Western blot; (D) Expression of TLR4 in lung tissue homogenates prepared from control and LPS-treated mice were analyzed by Western blot; (E) Expression of VCAM-1 in lung tissue homogenates prepared from control and LPS-treated mice were analyzed by Western blot; (F) Western blot showed that NF-κB and p-NF-κB expression in mouse lung tissue was significantly increased in the LPS group and further increased in the LPS+TFPI cKO group compared to the control group; statistically significant differences are denoted by asterisks: $^{*}P < 0.05$;$^{**}P < 0.01$; $^{***}P < 0.001$; $^{****}P < 0.0001$. ALI indicates acute lung injury; BALF, bronchoalveolar lavage fluid; LPS, lipopolysaccharide; PBS, phosphate buffer saline; TF, tissue factor; TFPI, tissue factor pathway inhibitor; TLR4, toll-like receptor 4; WT, wild-type; VCAM-1, vascular cell adhesion molecule 1.

expression increased significantly after the mice were treated with LPS for 48 h compared to the control group (Fig. 6, B and E). Following LPS administration, VCAM-1 protein was significantly expressed in the lungs of TFPI cKO mice compared to WT mice. Western blot revealed basal TLR4, p-NF-κB, and NF-κB levels in WT+PBS control groups; however, TLR4 and p-NF-κB was significantly increased in the LPS group (Fig. 6, B, D, and F). Moreover, we found that the amount of TLR4 and p-NF-κB was further increased in the TFPI cKO+LPS mice. In a word, further downregulated ACE2 expression and upregulated VCAM-1 expression in the lungs of LPS groups activated TLR4 and nuclear translocation of the p65 subunit of NF-κB in TFPI cKO mice, consistent with the results obtained from the immunoblot assay.

DISCUSSION

LPS is an effective proinflammatory agent that directly disrupts pulmonary endothelium barrier function in both macro- and microvascular ECs (20). LPS-induced murine lung injury is a disease model that shares many characteristics of sepsis-induced ALI/ARDS in humans. Functional alterations of pulmonary vascular endothelium cells play a critical role in the development of ALI/ARDS. Endothelial barrier dysfunction was evaluated by measuring transendothelial permeability, morphology, and LPS-activated inflammatory signaling pathways.

Coagulation and fibrinolysis abnormalities are also observed in ALI in both human disease and animal models, and may contribute to ongoing inflammation in the lungs. Given the extensive cross-talk between inflammation and coagulation, the observed diminishing effects on local coagulation may account for dampened pulmonary inflammation with nebulization of anticoagulants (21). Pulmonary coagulopathy is now accepted as a new target in the treatment of ALI/ARDS (1, 22). More than 40% of ALI patients have hematological dysfunction or disseminated intravascular coagulation, all of which are associated with higher mortality (23). We therefore investigated

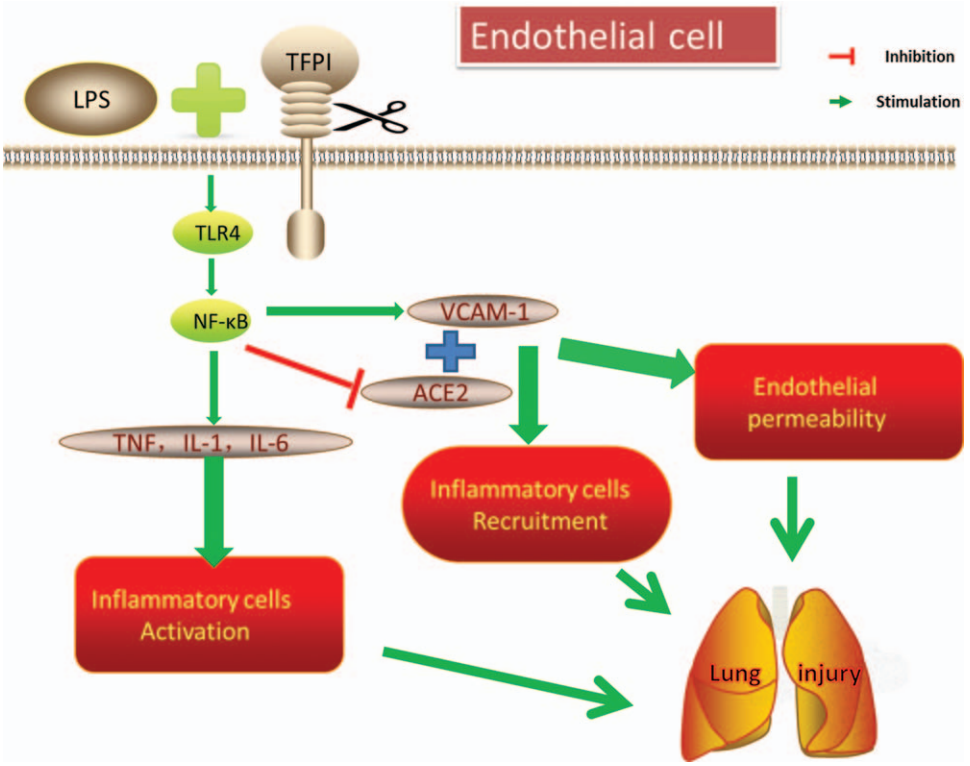

Fig. 7. **Diagram of knockdown of TFPI-anchored endothelial cells induced a more severe LPS-induced acute lung injury via NF-κB signaling pathway.** These results support the pro-inflammatory and barrier-destructive effects of endothelial-specific disruption of TFPI for septic inflammation and vascular endothelial barrier dysfunction in the TFPI cKO animal models of LPS-induced acute lung injury. LPS indicates lipopolysaccharide; TFPI, tissue factor pathway inhibitor.

coagulation status in the LPS-challenged model-directed lung injury through assessing coagulation in plasma.

Our results indicate that there were no significant differences in PT, APTT, and TT time in mice with LPS-induced lung injury via endotracheal intubation compared to controls. In our sample, TFPI plasma values in PBS controls and ALI groups were not significantly different; however, TFPI protein expression in lung tissue was significantly decreased after LPS administration. In addition, the TF expression in lung tissue was significantly increased. Increased activation of coagulation in the lungs has been reported, and is likely related to the formation of a TF-coagulation factor VII complex, which leads to thrombin generation and subsequently to fibrin formation (24). TFPI is attached to the endothelium via proteoglycans and regulates TF expression and activity, and is expressed primarily in ECs, the primary source of TFPI, and by the vascular endothelium of lung tissue (25).

In this study, endothelial-specific TFPI cKO mice were generated via Cre/LoxP and experiments were performed to investigate the involvement of TF and TFPI during ALI *in vivo*. TFPI concentrations in plasma and lungs from TFPI cKO mice with ALI were significantly lower than in WT mice. We also found that TFPI cKO mice with ALI exhibited increased vascular permeability, resulting in significantly aggravation of lung injury. Therefore, low levels of TFPI in mice are associated with increased severity of ALI after intratracheal LPS administration.

ACE2 is a membrane-associated aminopeptidase expressed in multiple lung cell types, including alveolar epithelial cells and ECs (26). Treatment with recombinant ACE2 also improved symptoms and attenuated arterial hypoxemia in a piglet model of LPS-induced ARDS (27). In this study, we evaluated ACE2 expression in the lungs and found that pulmonary ACE2 levels decreased significantly in mice with ALI and that ACE2 levels in TFPI cKO mice were lower than in WT mice after LPS administration. The acute phase of septic lung injury is characterized by increased vascular permeability, expression of adhesive surface molecules, such as VCAM-1, by activated EC. Several studies have demonstrated VCAM-1 expression in ECs and airway smooth muscle cells induced by LPS administration (28–30). Our study revealed that VCAM-1 expression increased significantly after mice were treated with LPS for 48 h; VCAM-1 was significantly expressed in the lung in TFPI cKO mice when compared to WT mice.

Previous studies have shown that the endotoxin receptor, TLR4 was found to mediate the early stages of the increased vascular permeability and inflammatory responses by LPS (31, 32). LPS-induced lung injury is associated with activation of NF-κB signaling pathways (33). The TLR4-mediated NF-κB cascade plays a pivotal role in the intracellular signaling pathway involved in vascular permeability and the inflammatory response, and activation of NF-κB is central to the regulation of pulmonary inflammation and the pathogenesis

of ARDS. In the present *in vivo* study, endothelial-specific disruption of TFPI markedly enhanced LPS-induced activation of NF-κB P65 phosphorylation expression, demonstrating that endothelial TFPI deletion may increase LPS-induced vascular permeability and inflammation via inhibition of the TLR4-mediated NF-κB pathway.

Protein expression of VCAM-1 is regulated by NF-κB activation, which is a proinflammatory transcription factor in the inflammatory response. Previous *in vitro* studies demonstrated that ACE2 prevented rat pulmonary microvascular ECs from LPS-induced apoptosis and inflammation by inhibiting activation of the NF-κB pathway. In this study, parallel trends were observed in the suppression of ACE2 expression and promotion of VCAM-1 expression and NF-κB activation in mice with ALI.

In this study, we provided experimental evidence to support that LPS-induced lung injury is associated with the TLR4-mediated NF-κB pathway (Fig. 7). We found further increased TLR4 and NF-κB activation in TFPI cKO mice compared to WT mice after LPS administration. VCAM-1 expression and reduced ACE2 expression were found in the TFPI cKO+LPS mice compared with WT+LPS mice. In addition, TNF-α, IL-1β, and IL-6 levels in TFPI cKO mice were also higher than in WT mice after LPS administration. Therefore, LPS via endotracheal instillation may induce a more serious ALI in TFPI cKO mice.

In conclusion, the present study, for the first time, used the LPS-induced lung injury mouse model to demonstrate that EC TFPI deficiency promotes LPS-induced pulmonary inflammation and vascular permeability and activates the TLR4-mediated NF-κB signaling pathway. We speculate that TFPI deficiency exacerbated lung injury after sepsis, suggesting that the presence of TFPI protects against ALI, possibly through TLR4-mediated NF-κB signaling pathway.

REFERENCES

1. Schultz MJ, Haitsma JJ, Zhang H, Slutsky AS: Pulmonary coagulopathy as a new target in therapeutic studies of acute lung injury or pneumonia—a review. *Crit Care Med* 34(3):871–877, 2006.
2. Katz JN, Kolappa KP, Becker RC: Beyond thrombosis: the versatile platelet in critical illness. *Chest* 139(3):658–668, 2011.
3. Welty-Wolf KE, Carraway MS, Ortel TL, Piantadosi CA: Coagulation and inflammation in acute lung injury. *Thromb Haemost* 88(1):17–25, 2002.
4. Eisenreich A, Rauch U: Regulation and differential role of the tissue factor isoforms in cardiovascular biology. *Trends Cardiovasc Med* 20(6):199–203, 2010.
5. Bastarache JA, Sebag SC, Clune JK, Grove BS, Lawson WE, Janz DR, Roberts LJ 2nd, Dworski R, Mackman N, Ware LB: Low levels of tissue factor lead to alveolar hemorrhage, potentiating murine acute lung injury and oxidative stress. *Thorax* 67(12):1032–1039, 2012.
6. Peterson JA, Maroney SA, Mast AE: Targeting TFPI for hemophilia treatment. *Thromb Res* 141(suppl 2):S28–S30, 2016.
7. Thomassen MC, Heinzmann AC, Herfs L, Hartmann R, Dockal M, Scheiflinger F, Hackeng TM, Rosing J: Tissue factor-independent inhibition of thrombin generation by tissue factor pathway inhibitor-α. *J Thromb Haemost* 13(1):92–100, 2015.
8. Maroney SA, Hansen KG, Mast AE: Cellular expression and biological activities of alternatively spliced forms of tissue factor pathway inhibitor. *Curr Opin Hematol* 20(5):403–409, 2013.
9. Levitt JE, Matthay MA: Clinical review: Early treatment of acute lung injury-paradigm shift toward prevention and treatment prior to respiratory failure. *Crit Care* 16(3):233, 2012.
10. Ma L, Shaver CM, Grove BS, Mitchell DB, Wickersham NE, Wickersham NE, Carnahan RH, Cooper TL, Brake BE, Ware LB, et al.: Kinetics of lung tissue factor expression and protocoagulant activity in bleomycin induced acute lung injury. *Clin Transl Med* 4(1):63, 2015.
11. Schirm S, Liu X, Jennings LL, Jedrzejewski P, Dai Y, Hardy S: Fragmented tissue factor pathway inhibitor (TFPI) and TFPI C-terminal peptides eliminate serum-resistant Escherichia coli from blood cultures. *J Infect Dis* 199(12):1807–1815, 2009.
12. Rancourt RC, Veress LA, Ahmad A, Hendry-Hofer TB, Rioux JS, Garlick RB, White CW: Tissue factor pathway inhibitor prevents airway obstruction, respiratory failure and death due to sulfur mustard analog inhalation. *Toxicol Appl Pharmacol* 272(1):86–95, 2013.
13. Abraham E, Reinhart K, Opal S, Demeyer I, Doig C, Rodriguez AL, Beale R, Svoboda P, Laterre PF, Simon S, et al.:, OPTIMIST Trial Study Group. Efficacy and safety of tifacogin (recombinant tissue factor pathway inhibitor) in severe spesis: a randomized controlled trial. *JAMA* 290(2):238–247, 2003.
14. Wang J, Xiao J, Wen D, Wu X, Mao Z, Zhang J, Ma D: Endothelial cell-anchored tissue factor pathway inhibitor regulates tumor metastasis to the lung in mice. *Mol Carcinog* 55(5):882–896, 2015.
15. Alame G, Mangin PH, Freund M, Riehl N, Magnenat S, Petitou M, Hechler B, Gachet C: EP217609, a neutralisable dual-action FIIa/FXa anticoagulant, with antithrombotic effects in arterial thrombosis. *Thromb Haemost* 113(2):385–395, 2015.
16. Murao Y, Loomis W, Wolf P, Hoyt DB, Junger WG: Effect of dose of hypertonic saline on its potential to prevent lung tissue damage in a mouse model of hemorrhagic shock. *Shock* 20(1):29–34, 2003.
17. Langheinrich AC, Leithäuser B, Greschus S, Von Gerlach S, Breithecker A, Matthias FR, Rau WS, Bohle RM: Acute rat lung injury: feasibility of assessment with micro-CT. *Radiology* 233(1):165–171, 2004.
18. Perez-Casal M, Downey C, Cutillas-Moreno B, Zuzel M, Fukudome K, Toh CH: Microparticle-associated endothelial protein C receptor and the induction of cytoprotective and anti-inflammatory effects. *Haematologica* 94(3):387–394, 2009.
19. Wang L, Li Y, Qin H, Xing D, Su J, Hu Z: Crosstalk between ACE2 and PLGF regulates vascular permeability during acute lung injury. *Am J Transl Res* 8(2):1246–1252, 2016.
20. Bogatcheva NV, Zemskova MA, Kovalenkov Y, Poirier C, Verin AD: Molecular mechanisms mediating protective effect of cAMP on lipopolysaccharide (LPS)-induced human lung microvascular endothelial cells (HLMVEC) hyperpermeability. *J Cell Physiol* 221(3):750–759, 2009.
21. Schultz MJ, Dixon B: A breathtaking and bloodcurdling story of coagulation and inflammation in acute lung injury. *J Thromb Haemost* 7(12):2050–2052, 2009.
22. Ware LB, Camerer E, Welty-Wolf K, Schultz MJ, Matthay MA: Bench to bedside: targeting coagulation and fibrinolysis in acute lung injury. *Am J Physiol Lung Cell Mol Physiol* 291(3):L307–L311, 2006.
23. Fujishima S, Gando S, Daizoh S, Kushimoto S, Ogura H, Mayumi T, Takuma K, Kotani J, Yamashita N, Tsuruta R, et al.:, Japanese Association for Acute Medicine Sepsis Registry (JAAM SR) Study Group. Infection site is predictive of outcome in acute lung injury associated with severe sepsis and septic shock. *Respirology* 21(5):898–904, 2016.
24. Bartko J, Schoergenhofer C, Schwameis M, Buchtele N, Wojta J, Schabbauer G, Stiebellehner L, Jilma B: Dexamethasone inhibits endotoxin-induced coagulopathy in human lungs. *J Thromb Haemost* 14(12):2471–2477, 2016.
25. Ramli J, CalderonArtero P, Block RC, Mousa SA: Novel therapeutic targets for preserving a healthy endothelium: strategies for reducing the risk of vascular and cardiovascular disease. *Cardiol J* 18(4):352–363, 2011.
26. Cao L, Xu L, Huang B, Wu L: Propofol increase angiotensin-converting enzyme 2 expression in human pulmonary artery endothelial cells. *Pharmacology* 95(5-6):342–347, 2012.
27. Treml B, Neu N, Kleinsasser A, Gritsch C, Finsterwalder T, Geiger R, Schuster M, Janzek E, Loibner H, Penninger J, et al.: Recombinant angiotensin-converting enzyme 2 improves pulmonary blood flow and oxygenation in lipopolysaccharide-induced lung injury in piglets. *Crit Care Med* 38(2):596–601, 2010.
28. Lazaar AL, Albelda SM, Pilewski JM, Brennan B, Puré E, Panettieri RA Jr: Tlymphocytes adhere to airway smooth muscle cells via integrins and CD44 and induce smooth muscle cell DNA synthesis. *J Exp Med* 180(3):807–816, 1994.
29. Cox LA, Van Eijk LT, Ramakers BP, Dorresteijn MJ, Gerretsen J, Kox M, Pickker P: Inflammation-induced increases in plasma endocan levels are associated with endothelial dysfunction in humans in vivo. *Shock* 43(4):322–326, 2015.
30. Uehara Y, Murata Y, Shiga S, Hosoi Y: NSAIDs diclofenac, indomethacin, and meloxicam highly upregulate expression of ICAM-1 and COX-2 induced by X-irradiation in human endothelial cells. *Biochem Biophys Res Commun* 479(4):847–852, 2016.

31. Mohammad T, Nebojsa K, Koteswara RC, Monica S, Sukriti S, Nicholas G, Alexander GO, Stephen MV, Dean ES, Alexander D, et al.: TLR4 activation of TRPC6-dependent calcium signaling mediates endotoxin-induced lung vascular permeability and inflammation. *J Exp Med* 209(11):1953–1968, 2012.
32. Andonegui G, Zhou H, Bullard D, Kelly MM, Mullaly SC, McDonald B, Long EM, Robbins SM, Kubes P: Mice that exclusively express TLR4 on endothelial cells can efficiently clear a lethal systemic Gram-negative bacterial infection. *J Clin Invest* 119(7):1921–1930, 2009.
33. Wang Y, Zhang A, Lu S, Pan X, Jia D, Yu W, Jiang Y, Li X, Wang X, Zhang J, et al.: Adenosine 5′-monophosphate-induced hypothermia inhibits the activation of ERK1/2, JNK, p38 and NF-kappaB in endotoxemic rats. *Int Immunopharmacol* 23(1):205–210, 2014.